Hyperfine Interact (2011) 203:105–112
DOI 10.1007/s10751-011-0351-3

Improving the empirical model for plasma nitrided AISI 316L corrosion resistance based on Mössbauer spectroscopy

M. Campos · S. D. de Souza · S. de Souza · M. Olzon-Dionysio

Published online: 30 August 2011

Abstract Traditional plasma nitriding treatments using temperatures ranging from approximately 650 to 730 K can improve wear, corrosion resistance and surface hardness on stainless steels. The nitrided layer consists of some iron nitrides: the cubic γ' phase (Fe_4N), the hexagonal phase ε ($Fe_{2-3}N$) and a nitrogen supersatured solid phase γ_N. An empirical model is proposed to explain the corrosion resistance of AISI 316L and ASTM F138 nitrided samples based on Mössbauer Spectroscopy results: the larger the ratio between ε and γ' phase fractions of the sample, the better its resistance corrosion is. In this work, this model is examined using some new results of AISI 316L samples, nitrided under the same previous conditions of gas composition and temperature, but at different pressure, for 3, 4 and 5 h. The sample nitrided for 4 h, whose value for ε/γ' is maximum ($= 0.73$), shows a slightly better response than the other two samples, nitrided for 5 and 3 h ($\varepsilon/\gamma' = 0.72$ and 0.59, respectively). Moreover, these samples show very similar behavior. Therefore, this set of samples was not suitable to test the empirical model. However, the comparison between the present results of potentiodynamic polarization curves and those obtained previously at 4 and 4.5 torr, could indicated that the corrosion resistance of the sample which only presents the γ_N phase was the worst of them. Moreover, the empirical model seems not to be ready to explain the response to corrosion and it should be improved including the γ_N phase.

Keywords AISI 316L · Mossbauer spectroscopy · Corrosion resistance · Empirical model

M. Campos · S. D. de Souza · M. Olzon-Dionysio (✉)
Departamento de Física, Universidade Federal de São Carlos, 13565-950, São Carlos, SP, Brazil
e-mail: dmod@df.ufscar.br

S. de Souza
Centro de Ciência e Tecnologia de Materiais, Instituto de Pesquisas Energéticas e Nucleares, 05508-000, São Paulo, SP, Brazil

1 Introduction

In spite of their good corrosion resistance in many aggressive environments, stainless steels show the effects of pitting corrosion in chloride ion solutions. Moreover, their industrial applications are limited because of the low hardness and low wear resistance. Traditional plasma nitriding treatments using treatment temperatures from approximately 650 to 730 K can improve the wear and corrosion resistance, as well as the surface hardness. The nitrided layer consists of some iron nitrides (f.c.c. γ' (Fe_4N) and hexagonal ε ($Fe_{2-3}N$)) and the metastable phase. This is known as expanded austenite γ_N, which is mainly responsible for improving nitrided AISI 316L properties [1] according to some authors. However, most of them use X-Ray Diffraction (XRD) in their studies. The difractograms present some difficulties, such as the enlargement of the γ_N peaks. Once γ'and ε peak positions are close to the γ_N peak positions, these phases can not be reliably identified. In recent studies on AISI 316L and ASTM F138 nitrided samples, we used not only XRD, but also Conversion Electron Mössbauer Spectroscopy (CEMS), as well as observing their corrosion resistance [2, 3]. As the phases show distinct hyperfine parameters, the Mössbauer spectra can provide better information. The results have demonstrated that the ε/γ' fraction ratio seemed to play an important role in the corrosion resistance as the best sample showed the maximum value for this ratio. Therefore, we proposed an empirical model. The larger this ratio value of the sample is, the better its corrosion resistance is. Some new results of AISI 316L samples, nitrided under the same conditions of gas composition and temperature, but at different pressures, are used in this work to examine the empirical model.

2 Materials and methods

AISI 316L stainless steel was produced by Villares Metals. It was annealed in the industry at 1323 K for 60 min and then cooled in water. Its chemical composition (in wt. %) is: 0.03% C, 17.0% Cr, 10. 0% Ni, 2.15% Mo and Fe balance. The samples (diameter, 19.70 mm, thick, 3.85 mm) were polished, cleaned ultrasonically in an acetone bath and finally air-dried. Afterwards, they were plasma nitrided in equipment with a DC power supply, which consists of a hermetically closed vessel containing two electrodes: an anode and a cathode, where the metallic work piece is placed. A nitriding atmosphere, consisting of a mixture of 20% N_2-80% H_2, at a pressure of 6 Torr was used. The voltage applied between the electrodes was adjusted at ≈400 V (and current density ≈485 mA) to maintain the temperature at 400°C. This was measured using an alumel–chromel (type K) long rod thermocouple placed underneath the sample. The samples were nitrided at different nitriding time intervals (t_N) of 3, 4, and 5 h.

The Mössbauer spectra of untreated and nitrided samples were obtained in the backscattering geometry using a conventional constant acceleration Mössbauer spectrometer. A self-built detection chamber was used with a 95% He + 5% CH_4 gas mixture flux. A ^{57}Co source in Rh matrix with a nominal activity of 100 mCi was used. The CEMS measurements were performed at room temperature and the isomer shifts were given relative to α-Fe.

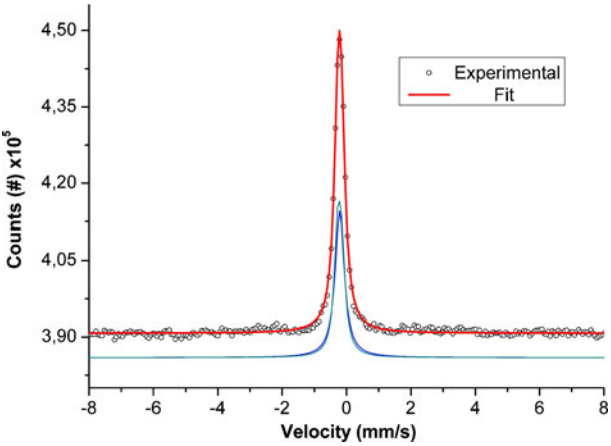

Fig. 1 CEMS spectra for the AISI 316L sample before nitriding

The corrosion performance of the samples was investigated in 3% NaCl aerated electrolytic solution using an Autolab PGSTAT30 Potentiostat/Galvanostat. Potentiodynamic polarization curves were obtained using the EG&G-Pal M352 Software. The scanning potential was in the range of -1.0 $V_{(SCE)}$ (cathodic potential) to $+0.8$ $V_{(SCE)}$ (anodic potential), and the scan rate was 1 mV s^{-1}. Electrochemical experiments were performed in a conventional Pyrex cell using untreated and nitrided AISI 316L samples as working electrodes and a platinum sheet as a counter electrode. The potentials were related to the saturated calomel electrode (SCE) in a KCl solution and all the electrochemical experiments were done at room temperature.

3 Results and discussion

The depth of the nitrided layer, measured in a Scanning Electron Microscopy, was in the range of 3.0 to 4.0 μm. Figure 1 shows the CEMS spectrum for the untreated sample. It shows that the surface of this sample is formed by 51% of an austenitic f.c.c. phase represented by one single-line (isomer shift IS = −0.09(1) mm/s). The remaining 49% was represented by one double-line component (IS = −0.09(1) mm/s and quadrupole splitting EQ = 0.13(1) mm/s), which means that the Fe atom neighbors affect the FCC cubic symmetry.

Figure 2a, b and c show the CEMS data for the nitrided samples. The spectra were fitted as a superposition of the sub-spectra of different phases: a nitrogen supersatured solid phase γ_N, a hexagonal ε phase and the γ' phase. Table 1 presents the Mössbauer parameters used for these different phases, which are in agreement with previous results [4–11].

Figure 3 shows the phase fractions obtained from the Mössbauer fittings as a function of t_N, where $\gamma_N = \gamma_N(p) + \gamma_N(m)$. The γ_N fraction stays constant at 40%. When t_N increases from 3 to 4 h, the ε phase concentration increases as well and the γ' phase concentration decreases. This is because the largest amount of nitrogen that is introduced should be used to transform the γ' phase into the ε phase, which

Table 1 Hyperfine parameters used to fit the different CEMS spectra for nitriding time of 3, 4, and 5 h. H is the magnetic hyperfine field, EQ is the quadruple splitting, IS is the isomer shift

Phase	H (T)	EQ (mm/s)	IS (mm/s)	Reference
γ_N(p)	–	–	-0.09 ± 0.05[b]	[4]
γ_N(m)	15.5	–	0.25	[5]
γ_N(m)	16.8	–	0.18	[6]
$\gamma'-Fe_4N$	21.8	–0.21	0.16	[7]
$\gamma'-Fe_4N$	34.2	–	0.35	[8]
$\varepsilon-Fe_{2,47}N$	–	0.86	0.31	[9]
$\varepsilon-Fe_{2,5}N$	25.6	–	0.12	[10]
$\varepsilon-Fe_{2,6}N$	–	0.68 ± 0.02[a]	0.39 ± 0.09[c]	[9]
$\varepsilon-Fe_3N$	28.8	–	0.09	[11]

[a]0.66 and 0.70 for 3 and 4 h

[b]−0.14, −0.14 and −0.04 for 3, 4 and 5 h

[c]0.47and 0.30 for 3 and 4 h

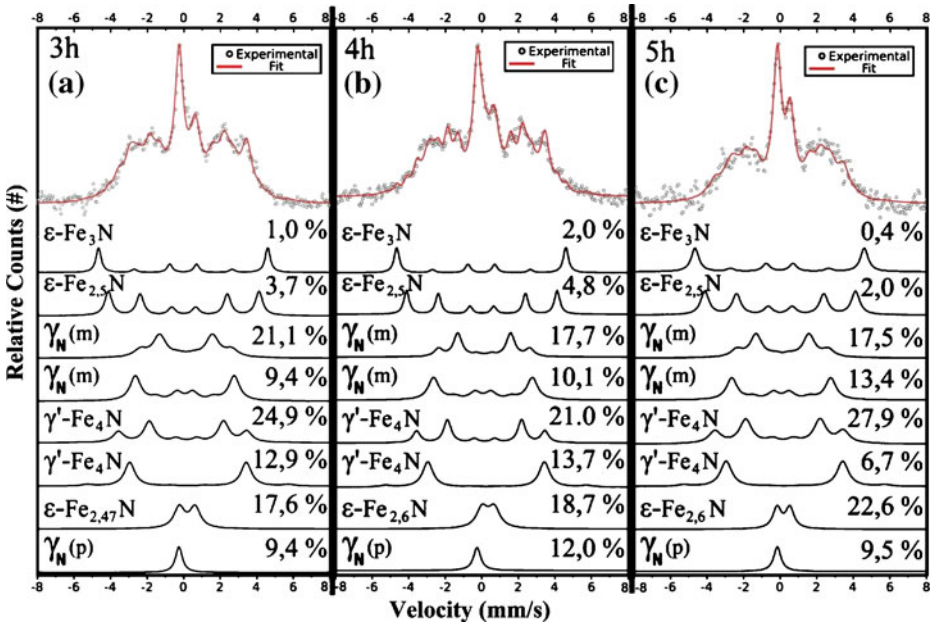

Fig. 2 **a–c** CEMS spectra for the AISI 316L samples nitrided at 3, 4 and 5 h

is richer in nitrogen. After 4 h, the system seems to come into equilibrium as the concentrations remain constant. The broad nature of the resonance signal is due to variations in the local N, Cr, Ni environments around Fe [12].

Figure 3 also shows the data from the reference [2], where we studied the same sample nitrided at the same temperature conditions, but at a pressure of 4.5 Torr. We can compare the time of 4 h, which was used in both studies. The concentration values of ε and γ' phases are very close in both studies. However, the value of the γ_N phase of this study is about 10% above that obtained previously, where we also

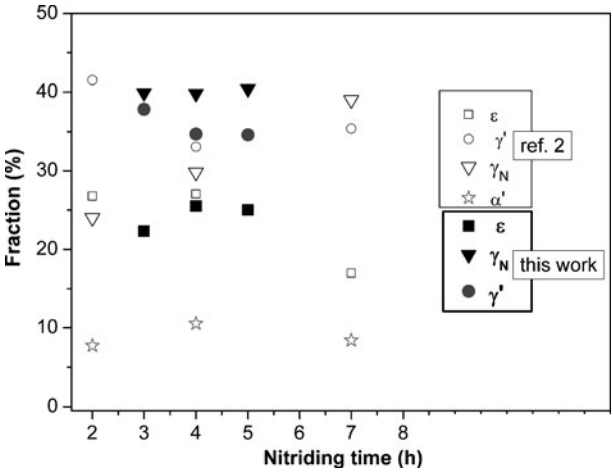

Fig. 3 Fractions of the adjusted phases as a function of different time intervals used during nitriding at 6 and 4.5 Torr [2]

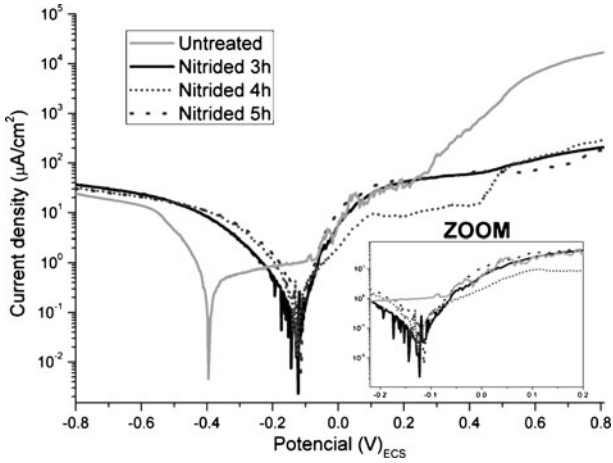

Fig. 4 Polarization curves in 3% NaCl aerated electrolytic solution of the ASIS 316L samples untreated and nitrided for 3, 4 and 5 h

observed the presence of about 10% of the martensite α' phase, formed on the near surface during mechanical polishing of the sample [13].

Figure 4 shows the potentiodynamic polarization curves for untreated and nitrided samples.

Although the sample nitrided for 4 h, whose value for ε/γ' is a maximum ($= 0.73$), has a slightly better response than the other two samples, nitrided for 5 and 3 h ($\varepsilon/\gamma' = 0.72$ and 0.59, respectively), these samples show very similar behavior. Therefore, this set of samples is not sufficient to test the empirical model.

It is interesting to compare the present corrosion results with some preceding ones [2, 14], where the samples were nitrided at 400°C for 4 h at 4.0 and 4.5 Torr. Figure 5(a) and (b) show the potentiodynamic polarization curves for untreated and nitrided samples for both studies.

All the nitrided samples show a higher corrosion potential (E_{corr}) compared to the untreated sample. The samples nitrided at 4.5 and 6 Torr, which have ε and

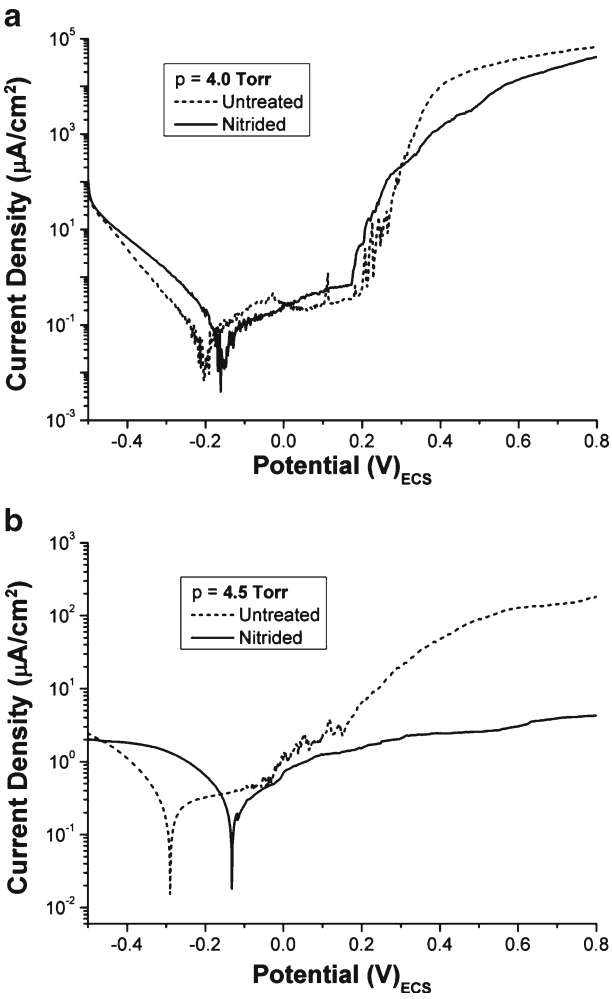

Fig. 5 Polarization curves in 3% NaCl aerated electrolytic solution of samples nitrited at **a** 4 Torr, **b** 4.5 Torr

γ' phases besides γ_N, showed a greater difference than the one nitrided at 4 Torr, which only has a γ_N phase. Indeed, an examination of the curve behavior shows that the sample nitrided at 4 Torr shows a rapid increase in current density, indicating localized corrosion, commonly known as pitting corrosion.

As is known, the lower the current density of the nitrided sample (j_{nitr}), in relation to the current of the untreated sample (j_{untr}), the better the corrosion resistance is. Therefore, to compare the nitrided sample response, it is appropriate to compare the ratio j_{nitr} /j_{untr} along the curve for the three studies. These values are given in Table 2.

Some authors [1] have regarded the presence of the γ_N phase as being responsible for better corrosion resistance. However, this comparison shows that the sample which presents only this phase was the worst. We now compare the values in the Table 2 for the sample nitrided at 4.5 Torr in [2], which shows the highest value for ε/γ'(=0.84), with the values for the three samples in this work. It can be observed that [2] sample is more resistant to corrosion than the samples nitrided at $t_N = 3$

Table 2 Ratio between current density of nitrided sample (j_{nitr}), in relation to the current of untreated sample (j_{untr}) along the polarization curve of the samples nitrided at different pressures [2, 14] and times

Sample	ε/γ'	j_{nit}/j_{untr} $E = 0.0$V	j_{nit}/j_{untr} $E = 0.1$V	j_{nit}/j_{untr} $E = 0.2$V	j_{nit}/j_{untr} $E = 0.3$V	j_{nit}/j_{untr} $E = 0.4$V	j_{nit}/j_{untr} $E = 0.5$V	j_{nit}/j_{untr} $E = 0.6$V
[14]	–(Only γ_N phase)	2.55	5.12	10.47	1.23	0.098	0.061	0.064
[2]	0.84	0.57	0.58	0.23	0.10	0.051	0.028	0.024
This work								
3h	0.59	0.87	0.99	1.27	0.38	0.13	0.039	0.018
4h	0.73	0.43	0.46	0.28	0.12	0.031	0.036	0.022
5h	0.72	1.58	1.38	1.32	0.38	0.13	0.032	0.011

and 5h. On the other hand, if we compare the values of second (ref. [2] sample) with fourth ($t_N = 4$h) rows in Table 2, it is difficult to choose the best one. However, Fig. 4 shows that the passive region (in the range between 0.14 and 0.43 V) is better defined for sample nitrided at 4h, than for sample nitrided at 4.5 Torr (Fig. 5b). In this region, the second row shows values which are slightly lower than those in fourth row. It indicates that the sample in [2] seems to be a little more resistant than the sample nitrided at 4h. Thus, it can be concluded that this empirical model is not yet ready to explain the response to corrosion. It is very likely that the γ_N phase also has an important role in the corrosion process and this model should be improved also including the γ_N phase. We are currently developing a systematic study using a higher number of samples with this aim.

4 Conclusions

The AISI 316L samples nitrided for 3, 4 and 5 h, at 6 Torr showed the presence of three phases: ε, γ' and γ_N. The proportions of these phases were used to examine the empirical model which correlates the maximum ratio ε/γ' with the best corrosion resistance. The sample nitrided for 4 h, whose value for ε/γ' is maximum ($= 0.73$), shows a slightly better response than the other two samples, nitrided for 5 and 3 h ($\varepsilon/\gamma' = 0.72$ and 0.59, respectively). Moreover, these samples show very similar behavior. Therefore, this set of samples was not sufficient to test the empirical model.

However, the comparison between the present results of potentiodynamic polarization curves and those obtained previously at 4 and 4.5 torr, could indicated that: 1) the corrosion resistance of the sample which only presents the γ_N phase was the worst of them, 2) the empirical model is not yet ready to explain the response to corrosion and it should be improved including the γ_N phase.

Acknowledgements The Brazilian agencies FAPESP (Fundação de Amparo e Pesquisa do Estado de São Paulo) and CAPES(Coordenação de Aperfeiçoamento de Pessoal de Nível Superior) gave financial support for this investigation.

References

1. Fossati, A., Borgioli, F., Galvanetto, E., Bacci, T.: Corrosion resistance properties of glow-discharge nitrided AISI 316L austenitic stainless steel in NaCl solutions. Corros. Sci. **48**, 1513–1527 (2006)
2. Olzon-Dionysio, M., de Souza, S.D., Basso, R.L.O., de Souza, S.: Application of Mössbauer spectroscopy to the study of corrosion resistance in NaCl solution of plasma nitrided AISI 316L stainless steel. Surf. Coat. Technol. **202**, 3607–3614 (2008)
3. de Souza, S.D., Olzon-Dionysio, M., Basso, R.L.O., de Souza, S.: Mössbauer spectroscopy study on the corrosion resitance of plasma nitrided ASTM F138 stainless steel in chloride solution. Mater. Charact. **61**, 992–999 (2010)
4. Jiràsková, Y., Havlíček, S., Schneeweiss, O., Peřina, V., Blawert, C.: Characterization of iron nitrides prepared by spark erosion, plasma nitriding, and plasma immersion ion implantation. J. Magn. Magn. Mater. **234**, 477–488 (2001)
5. Ozturk, O., Williamson, D.L.: Phase and composition depth distribution analyses of low energy, high flux N implanted stainless steel. J. Appl. Phys. **77**, 3839–3850 (1995)
6. Gontijo, L.C., Machado, R., Miola, E.J., Casteletti, L.C., Alcântara, N.G., Nascente, P.A.P.: Study of the S phase formed on plasma-nitrided AISI 316L stainless steel. Mater. Sci. Eng. A **431**, 315–321 (2006)
7. Kuhnen, C.A., de Figueiredo, R. S. , Drago, V., da Silva, E. Z. : Mössbauer studies and electronic structure of γ'-Fe4N. J. Magn. Magn. Mat. **111**, 95–104 (1992)
8. Nozik, A.J., Wood Jr., J.C., Haacke, G.: High resolution Mössbauer spectrum of Fe_4N. Sol. St. Comm. **7**, 1677–1679 (1969)
9. Firrao, D., Rosso, M., Principi, G., Frattini, R.: The Influence of carbon on nitrogen Substitution in iron ε-phases. J. Math. Sci. **17**, 1773–1788 (1982)
10. Mekata, M., Yoshimura, H., Takaki, H.: Magnetic study on hexagonal nitrides of 3d transition metals. J. Phys. Soc. Jpn. **33**, 62–69 (1972)
11. DeCristofaro, N., Kaplow, R.: Mössbauer spectroscopy of hexagonal iron-nitrogen alloys. Metall. Mater. Trans. A **8**, 425–430 (1977)
12. Ozturk, O., Williamson, D.L.: Thermal stability of the high-N solid-solution layer on stainless steel. Surf. Coat. Technol. **158–159**, 288–294 (2002)
13. Wang, L., Xu, X., Xu, B., Yu, Z., Hei, Z.: Low temperature nitriding and carburizing of AISI304 stainless steel by a low pressure plasma arc source. Surf. Coat. Technol. **131**, 563–567 (2000)
14. Olzon-Dionysio, M., Campos, M., Kapp, M., de Souza, S., de Souza, S.D.: Influences of plasma nitriding edge effect on properties of 316L stainless steel. Surf. Coat. Technol. **204**, 3623–3628 (2010)